Bioconjugate Chemistry

Article

pubs.acs.org/bc

Growth Factor Tethering to Protein Nanoparticles via Coiled-Coil Formation for Targeted Drug Delivery

Yasmine Assal, Yoshinori Mizuguchi, Masayasu Mie, and Eiry Kobatake*

Department of Environmental Chemistry and Engineering, Interdisciplinary Graduate School of Science and Engineering, Tokyo Institute of Technology, Yokohama 226-8052, Japan

Supporting Information

ABSTRACT: Protein-based nanoparticles are attractive carriers for drug delivery because they are biodegradable and can be genetically designed. Moreover, modification of protein-based nanoparticles with cell-specific ligands allows for active targeting abilities. Previously, we developed protein nanoparticles comprising genetically engineered elastin-like polypeptides (ELPs) with fused polyaspartic acid tails (ELP-D). Epidermal growth factor (EGF) was displayed on the surface of the ELP-D nanoparticles via genetic design to allow for active cell-targeting abilities. Herein, we focused on the coiled-coil structural motif as a means for noncovalent tethering of growth factor to ELP-D. Specifically, two peptides known to form a heterodimer via a coiled-coil structural motif were fused to ELP-D and single-chain vascular endothelial growth factor ($scVEGF_{121}$), to facilitate noncovalent tethering upon formation of the heterodimer coiled-coil structure. Drug-loaded growth factor-tethered ELP-Ds were found to be effective against cancer cells by provoking cell apoptosis. These results demonstrate that tethering growth factor to protein nanoparticles through coiled-coil formation yields a promising biomaterial candidate for targeted drug delivery.

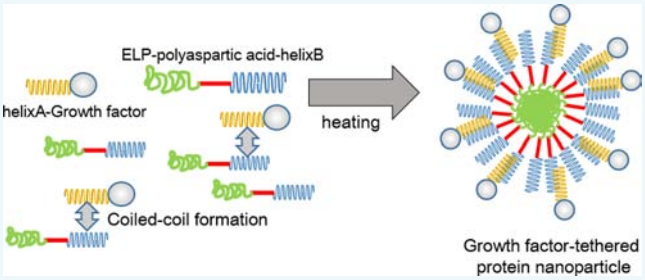

INTRODUCTION

Design of drug carriers is one of the most important efforts in the field of drug delivery system (DDS) development, as carriers are required to exhibit a number of properties such as high stability, low antigenicity, and greater accumulation in tumors than free drug. To satisfy such requirements, protein-based materials have been a focus for the design and development of DDSs.

Elastin-like polypeptides (ELPs) are often used in the design of drug delivery carriers owing to their biocompatibility, in vivo stability, and drug loading capacities.[1−3] Moreover, ELPs can form temperature-dependent aggregates above a transition temperature.[4] By controlling the size of such aggregates, we and others have developed ELP-based nanoparticles.[5,6] Our designed ELP-based nanoparticle system was composed of genetically engineered ELPs with fused poly(aspartic acid) tails (ELP-D). The sizes of the self-assembled ELP-D nanoparticles were regulated by charge repulsion of the poly(aspartic acid) chains. In addition, epidermal growth factor (EGF) was genetically fused to ELP-D to allow for cell-targeting abilities.[7]

In general, conjugation of cell-targeting protein or peptide ligands to drug vehicles requires chemical modifications. However, site selectivity and stoichiometry are difficult to control using chemical modifications. Genetic engineering can overcome such problems. We have previously demonstrated success in developing EGF-displaying protein-based nanoparticles that exhibit active tumor-targeting abilities. However, genetically engineered nanoparticles also exhibit problems, such as size limitation for expression of proteins and steric hindrance of the fused proteins used for the formation of nanoparticles. To overcome such problems, our group has focused on the use of peptides forming coiled-coil structures to allow for noncovalent tethering of growth factors to protein nanoparticles.

The coiled-coil structure is a well-understood protein motif found naturally in proteins. Various de novo-designed peptides forming coiled-coil structures have been synthesized and characterized.[8] Several de novo-designed coiled-coil peptides have been used for various applications, such as tissue engineering[9,10] and design of DDSs.[11−13] In the field of tissue engineering, Boucher et al. used de novo-designed peptides forming coiled-coil interactions for conjugation of EGF to polyethylene terephthalate. Previously, we constructed growth factor-tethered artificial extracellular matrix (ECM) proteins via coiled-coil formation.[14−16] In those studies, growth factors and ECM proteins were genetically fused with ACID-p1 (helix A) and BASE-p1 (helix B) peptides, respectively. These peptides, designed by O'Shea et al., form stable, parallel, coiled-coil heterodimers with a leucine zipper, and exhibit favorable electrostatic interactions.[17,18] Thus, our previous studies suggest that growth factors can be immobilized on ECM proteins through noncovalent bonding interactions. Pechar and

Received: May 11, 2015
Revised: June 15, 2015
Published: June 16, 2015

DOI: 10.1021/acs.bioconjchem.5b00266
Bioconjugate Chem. 2015, 26, 1672−1677

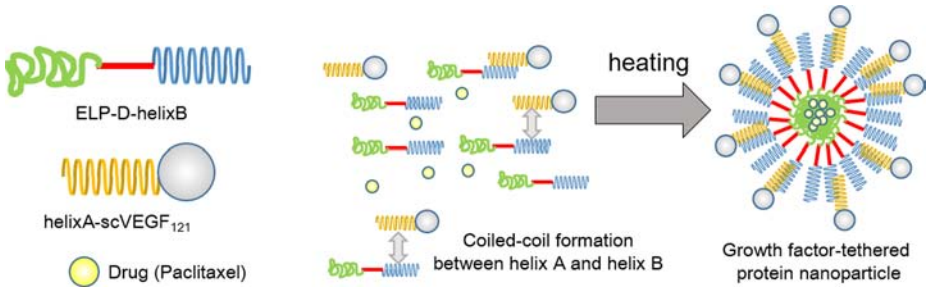

Figure 1. Schematic illustration of a growth factor-tethered protein nanoparticle via coiled-coil formation.

colleagues designed coiled-coil peptides as a tool for noncovalent binding between proteins and a synthetic drug carrier, and suggested the use of coiled-coil motifs as a universal tool to bind recombinant proteins to synthetic hydrophilic polymers.[11−13]

In this study, we developed a growth factor-tethered protein nanoparticle system utilizing coiled-coil formation to noncovalently tether growth factors to protein nanoparticles (Figure 1). To facilitate tethering via coiled-coil formation, helix A was genetically fused to the growth factor while helix B was fused to ELP-D. Here, we used a single-chain vascular endothelial growth factor ($scVEGF_{121}$) for the targeting VEGF receptor of cancer cells.[19] Following formation of VEGF-tethered ELP-D protein nanoparticles, the anticancer drug paclitaxel was loaded into the nanoparticles, and the effects on cancer cells were investigated.

RESULTS

Expression of Fusion Proteins. The tethering growth factor, helixA-$scVEGF_{121}$, was previously constructed in our lab.[15] The $scVEGF_{121}$ motif was shown to retain its ability to induce endothelial cell proliferation even after fusion with helix A. The protein was expressed in *E. coli* and purified from the insoluble faction using a Histidine tag.

For tethering helixA-$scVEGF_{121}$ to ELP-based nanoparticles through coiled-coil formation, BASE-p1 (helix B) peptide was fused to the C-terminus of $(PAVGV)_{42}$-D_{44}-CHis (ELP-D) fusion proteins (Figure 2A). The resulting fusion protein, $(PAVGV)_{42}$-D_{44}-helixB-CHis (ELP-D-helixB), contained 4 repeats of the GGGS sequence inserted as a linker between the poly(aspartic acid) chain and the helix B peptide. The ELP-D-helixB and ELP-D proteins were expressed in *E. coli* and purified from the soluble fraction using a Histidine tag at C-terminus (CHis). The purity of the fusion proteins was analyzed with SDS-PAGE (Figure 2B). The bands appeared larger than the expected molecular sizes (ELP-D: 26.7 kDa and ELP-D-helixB: 31.5 kDa). This expression behavior has previously been confirmed for ELPs.[20]

Characterization of ELP-Based Protein Nanoparticles. The thermal transition temperatures of ELP-D and ELP-D-helixB were evaluated. Proteins were heated from 20 to 50 °C, and subsequently cooled to 20 °C with a temperature gradient of 1 °C/min. The results of temperature turbidity are plotted in Figure 3A. Phase transition temperature measurements of ELP-D and ELP-D-helixB showed an abrupt increase in absorbance corresponding to the onset of turbidity, suggesting the formation of protein nanoparticles. Both proteins exhibited thermal transitions around 35 °C. The average diameter of the ELP-based protein nanoparticles was determined by dynamic light scattering (DLS) measurements (Figure 3B). Nanoparticle

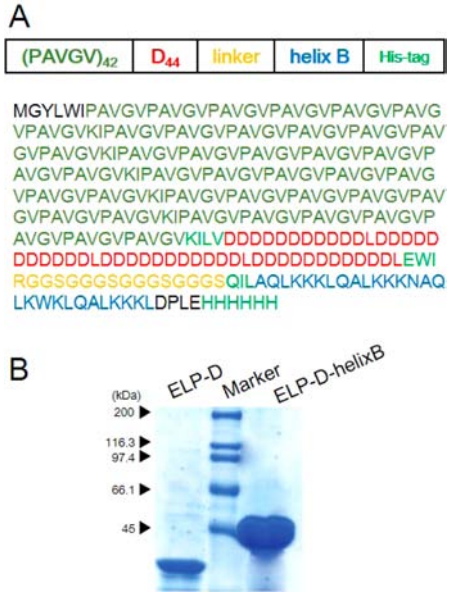

Figure 2. Expression and purification of ELP-D and ELP-D-helixB. (A) Construction of ELP-D-helixB and its amino acid sequence. (B) Purified ELP-D and ELP-D-helixB proteins.

sizes were measured at 25 °C, 50 °C, and again at 25 °C. At 25 °C, ELP-D and ELP-D-helixB particles showed peaks corresponding to diameters of approximately 8 and 12 nm, respectively. At 50 °C, a peak was observed between 30 and 35 nm for both ELP-D and ELP-D-helixB. After cooling to 25 °C, particle sizes of both protein particles remained nearly the same as at 50 °C. Size distribution measurements showed that both ELP-D and ELP-D-helixB maintained nanoparticle forms upon cooling. Figure 3C shows transmission electron microscopy (TEM) images of the ELP-D and ELP-D-helixB nanoparticles. TEM images show the presence of multiple nanoparticles at 50 °C, while only a few nanoparticles were observed at 25 °C. The ELP-D-helixB nanoparticle core size is approximately 30 ± 2 nm in diameter, as estimated from statistical analyses of the previous analysis. Taken together, TEM results confirm that the addition of helix B peptide did not impede the formation of nanoparticles or alter their structures.

Encapsulation of 1,8-ANS into ELP-Based Nanoparticles. The potential for encapsulation of drugs within the hydrophobic core of the ELP-D and ELP-D-helixB nanoparticles was investigated using the fluorescent probe 1,8-ANS (Figure 4). 1,8-ANS exhibits the ability to bind to the hydrophobic region of a protein, resulting in a blue shift of its emission peak and an increase in fluorescence intensity.[21,22] The proteins were mixed with 1,8-ANS followed by incubation at 25 °C. The emission peaks for both ELP-D and ELP-D-

DOI: 10.1021/acs.bioconjchem.5b00266
Bioconjugate Chem. 2015, 26, 1672−1677

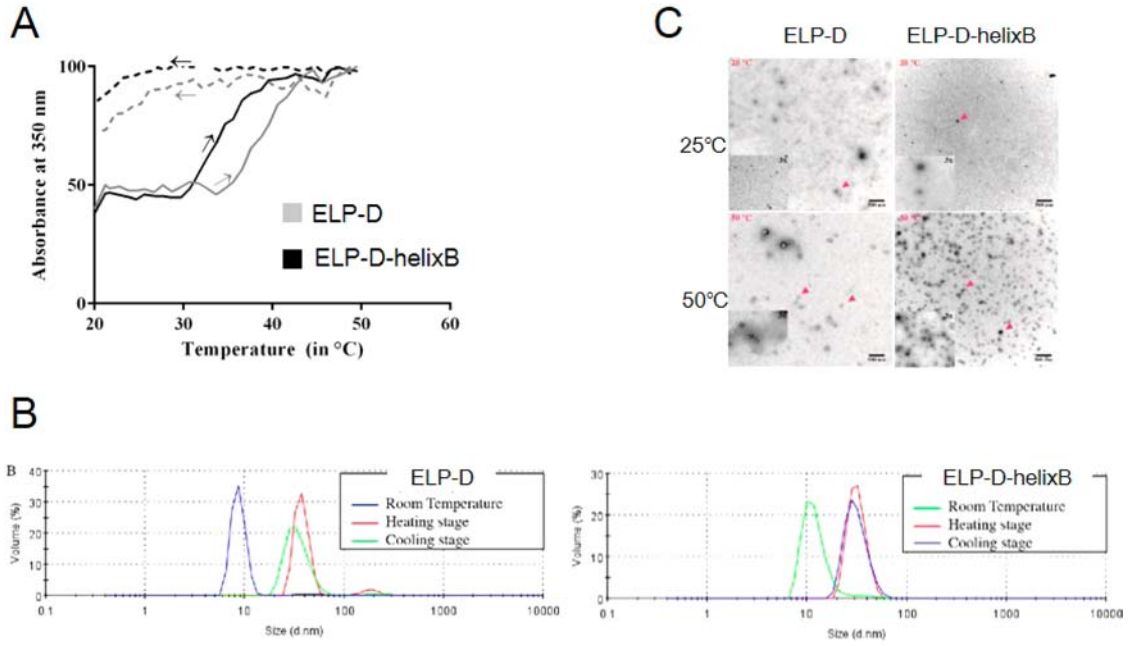

Figure 3. Characterization of ELP-D and ELP-D-helixB nanoparticles: (A) Turbidity (OD350) of ELP-D and ELP-D-helixB. The turbidity profiles of the polypeptides were obtained at a rate of 1 °C/min. Heating and cooling profiles were marked by arrows. (B) Hydrodynamic size distributions of ELP-D and ELP-D-helixB nanoparticles determined using dynamic light scattering. The number-average distribution (peak) indicates the average diameter of the nanoparticles. (C) Transmission electron microscopy (TEM) images of ELP-D and ELP-D-helixB nanoparticles at 25 and 50 °C. Arrowheads indicate nanoparticles.

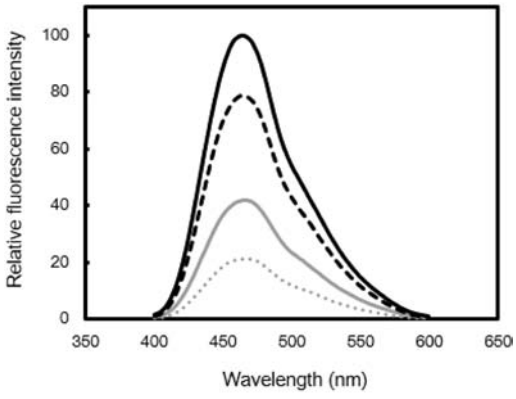

Figure 4. Fluorescence emission spectra of proteins (ELP-D-helixB (black) and ELP-D (gray)) mixed with 1,8-ANS at 50 °C (solid line) and at 25 °C (broken line) after cooling.

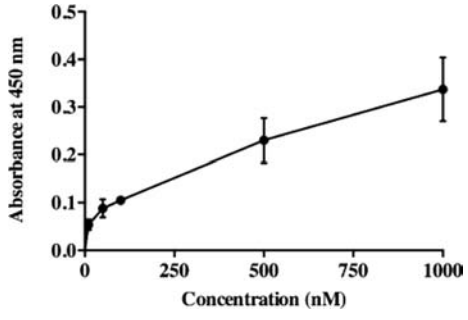

Figure 5. Binding of helixA-scVEGF$_{121}$ to ELP-D-helixB through coiled-coil structure on ELISA plate. Various concentrations of helixA-scVEGF$_{121}$ were reacted with ELP-D-helixB adsorbed onto 96-well plate surface.

helixB were nearly the same as that of 1,8-ANS at 25 °C (data not shown). After incubation at 50 °C, the intensity of the emission peaks was significantly increased. Upon cooling to 25 °C, the emission peaks were still more intense than that of 1,8-ANS. These results demonstrate that ELP-based nanoparticles exhibit the ability to encapsulate potential drugs upon heat treatment.

Protein Binding through the Coiled-Coil Structure. To examine the binding of helixA-scVEGF$_{121}$ to ELP-D-helixB, ELISA analysis was performed. Anti-VEGF antibody was used, and the signals were detected with horseradish peroxidase (HRP)-conjugated secondary antibody. Results show that the signal increased in a dose-dependent manner up to 1 μM (Figure 5), suggesting that noncovalent binding via coiled–coiled structure formation could function as an effective bridge connecting growth factors and protein nanoparticles.

In Vitro Evaluation of Paclitaxel-Loaded Nanoparticles via a Coiled-Coil Complex. To monitor the effect of paclitaxel (PTX)-loaded protein nanoparticles on HeLa cells and the progress of apoptosis, calcein-AM (Calcein) and propidium iodide (PI) staining were applied (Figure 6). Untreated HeLa cells showed no evidence of cell death at 2 days after staining with Calcein and PI, while cells treated with PTX were induced cell death and flushed away from dish because of cell death. Cells treated with PTX-loaded ELP-D-helixB nanoparticles and PTX-loaded ELP-D-VEGF nanoparticles were stained with both PI and Calcein. However, almost all cells treated with PTX-loaded ELP-D-VEGF nanoparticle were detached from the dish as well as the positive control. These results suggested that VEGF-tethering PTX-loaded ELP-D-helixB nanoparticles were internalized via binding to VEGF receptor and proved specific delivery of protein nanoparticles.

DOI: 10.1021/acs.bioconjchem.5b00266
Bioconjugate Chem. 2015, 26, 1672–1677

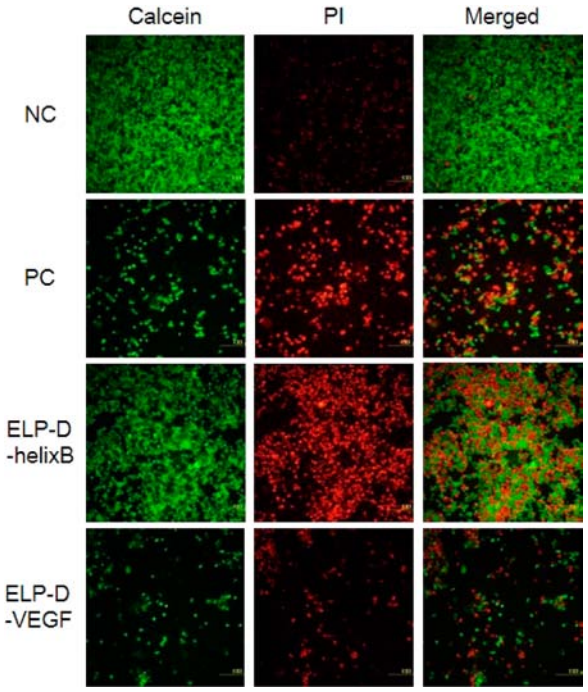

Figure 6. Effects of paclitaxel (PTX)-loaded protein nanoparticles on HeLa cells at 2 days after drug delivery. Fluorescent images showing calcein-AM (Calcein) and propidium iodide (PI) staining of cultured HeLa cells treated with PTX-loaded protein nanoparticles, scVEGF tethering ELP-D-helixB nanoparticle (ELP-D-VEGF), and nontethering ELP-D-helixB nanoparticle. Cells treated with PTX (10 μM) as positive control (PC). Untreated cells were expressed as negative control (NC).

DISCUSSION

In this study, we sought to design an ELP fused with an α-helix peptide (helix B) to favor heterodimer formation when combined with another α-helix peptide (helix A) fused with a growth factor, helixA-scVEGF$_{121}$, which was previously constructed in our lab.[14−16] ELP fused with a polyaspartic acid sequence and helix B at its C-terminus was found to form nanoparticles. The formation of nanoparticles states of the nanoparticles appear to respond under changes in temperature. Moreover, the ability to encapsulate small molecules and drugs seems to occur at the phase transition temperature. Noncovalent tethering of helixA-scVEGF$_{121}$ to the protein nanoparticles allowed for tumor-targeted drug delivery.[15]

The results of turbidimetry and DLS measurements revealed the formation of ELP-D-helixB nanoparticles. The suspension of ELP-D and ELP-D-helixB particles may have been hampered by a deficiency of water molecules around the amide groups, promoting stabilization of the nanoparticle formation.[23] The slow aggregation and disaggregation kinetics of ELP-D explain the difference in paths between the ELP-D and ELP-D-helixB traces, which may be caused by the addition of the helix B fragment to the original ELP-D backbone.[24]

To corroborate previously established findings, 1,8-ANS was loaded into ELP-D-helixB nanoparticles to demonstrate their potency in encapsulating drugs within their respective cores. Fluorescent probes, such as 1,8-ANS, register emission intensity in the presence of hydrophobic surfaces within tightly folded proteins.[25−27] In our previous experiments, 1,8-ANS incubated with bovine serum albumin did not result in a fluorescence spectra even upon changing the temperature.[5,7] In this study, a strong increase in the fluorescence intensity of the mixture of 1,8-ANS and ELP-D-helixB was observed at 50 °C compared with 25 °C (Figure 4). These results suggest that ELP-D-helixB particles encapsulated drugs within their respective cores. In addition, relatively high fluorescence emissions were recorded following cooling; however, they remained slightly lower than those at 50 °C. In both cases, the fluorescence intensity of ELP-D was somewhat lower than that of ELP-D-helixB. TEM images suggest only a small fraction of proteins formed nanoparticles at 25 °C. After heating, however, spherical-shaped granulations were formed (Figure 3C). The additional helix B sequence added to ELP-D did not impede the activity of nanoparticle formation, nor their thermoresponsive properties.

To confirm the efficacy of our noncovalent tethering strategy, we focused on VEGF as a tumor-targeting ligand. VEGF signaling in the pathological pathway is regulated by VEGF receptors. Our hypothesis suggests that nanoparticles are recognized by VEGF receptors through helixA-scVEGF$_{121}$, and that nanoparticle uptake by HeLa cells leads to PTX release and subsequent induction of cell death. Cell staining results demonstrate that cells treated with PTX-loaded ELP-D-VEGF showed considerable cell death only 6 h after treatment and almost all cells were dead at 12 h similar to positive control in which PTX was directly applied to the cells (Supporting Information Figure S1). The VEGF-tethering PTX-loaded nanoparticles were internalized via VEGF receptor and released PTX. This resulted in significant cell death, as noted by cell detachment from the tissue culture plate and subsequent removal from the cell media following a washing phase. These results confirm that VEGF and its receptors are good candidates for cancer therapy applications,[28] while cells treated with ELP-D-VEGF without PTX loading were not induced cell death the same as the negative control. This proved that ELP-D-VEGF does no harm to cells. The low cell death number recorded upon ELP-D-helixB application is due to nonspecific attachment of nanoparticles to the cell surface; therefore, the induction of cell death was delayed compared to cells treated with ELP-D-VEGF. Furthermore, the combination of coiled-coil heterodimers with targeted drug delivery may facilitate tumor suppression and induce apoptotic cell death, which would explain the significant cell detachment observed in this study.

CONCLUSION

We have successfully developed a new approach for targeted drug delivery and controlled release using ELP-based thermoresponsive nanoparticles noncovalently bound to growth factor. The nanoparticles were shown to effectively deliver PTX to cells, resulting in cell death and detachment. Taken together, this study demonstrates that customized DDSs, with regard to cell type and receptor, can be constructed. This new strategy introduces a promising biomaterial for customized drug delivery.

MATERIALS AND METHODS

Plasmid Construction. The plasmid pET28b-(PAVGV)$_{42}$-D$_{44}$-CHis was constructed in our previous experiment.[7] For construction of pET28b-(PAVGV)$_{42}$-D$_{44}$-helixB-CHis, helix B fragment with linker from pET-GGGS$_4$-helixB previously constructed in our laboratory was amplified by PCR using a pair of primers containing *Xho* I restriction enzymes sites (5′-AAGCTTCTCGAGTGGATCCGCGGTGGA-3′) and (5′-

DOI: 10.1021/acs.bioconjchem.5b00266
Bioconjugate Chem. 2015, 26, 1672−1677

AAGCTTCTCGAGTGGATCTAACTTTTTC-3′), and was then inserted into pBluescript II SK(+) followed by sequencing. To obtain $GGGS_4$-helixB fragment, pBS-$GGGS_4$-helixB was digested with *Xho* I. The obtained fragment was inserted into pET28b-$(PAVGV)_{42}$-D_{44}-CHis digested with the same restriction enzyme.

Expression and Purification of Fusion Proteins. For expression of proteins, ELP-D and ELP-D-helixB, pET28b-$(PAVGV)_{42}$-D_{44}-CHis, and pET28b-$(PAVGV)_{42}$-D_{44}-helixB-CHis plasmids were transfected into *E. coli* KRX competent cells by heat shock and cultured at 37 °C in a Luria−Bertani (LB) medium supplemented with ampicillin to an optical density of 0.6 at 600 nm. Protein expression was induced by addition of 1 mM IPTG and 0.1% rhamnose. Cells were cultured overnight at 30 °C, harvested by centrifugation (9000 *g*) and resuspended in Bug Buster Reagent and Benzonase nuclease followed by rotation at room temperature for 30 min before repelleting by centrifugation (9000 *g*) for 10 min. The supernatant was collected and purified by TALON Metal Affinity Resin (Clontech) using a Poly prep column (Bio-Rad). After 30 min incubation at 4 °C, the column was washed three times with four column volumes of the wash buffer (50 mM sodium phosphate, 300 mM NaCl, pH 7.6) followed by three times with four column volumes of the same buffer including 5 and 10 mM imidazole each. The fusion proteins were eluted with two column volumes of elution buffer (50 mM sodium phosphate, 300 mM NaCl, 100 mM imidazole, pH 7.6). The fusion proteins were then dialyzed in a PBS buffer overnight using a Slider-A-lyzer dialysis cassette (PIERCE).

Expression and purification of helixA-scVEGF$_{121}$ protein were performed following our previous paper.[15]

Turbidimetry. The optical density of the aqueous polymer solutions was monitored at 350 nm with a temperature-controlled UV/vis spectrophotometer (DU7500, Beckman Coulter). Proteins and reagents were filtered using a 0.22 μm filter (Millipore). All spectroscopic measurements were performed in quartz glass cuvettes. The starting temperature was set at 20 °C to slowly increase by 1 °C/min to a final temperature of 50 °C. Reverse measurement was also monitored. The concentration of the proteins applied was 200 μg/mL.

Dynamic Light Scattering Measurements. The size of the ELP-D and ELP-D-helixB nanoparticles formed in dilute aqueous solutions at 25 and 50 °C were determined by means of a NanoZetasizer, Nano-ZS Malvern apparatus. PBS was filtered through a 0.22 μm filter. The proteins were diluted with the filtered PBS to a final concentration of 500 μg/mL. Proteins were flowed into the flow cell to determine the nanoparticle size. Light scattering measurements were taken for 10 runs of 10 s. The excitation light source was a 4 mW He−Ne laser at 633 nm, and the intensity of the scattered light was measured at 90°. The sizes of the proteins were calculated based on the assumption that the viscosity of PBS was the same as that of water. The size with single-peaked distribution of the nanoparticles was determined by the cumulant algorithm software.

Transmission Electron Microscopy (TEM). TEM samples were diluted and dissolved in filtered PBS to a final concentration of 300 μg/mL. Particle fixation involved incubation of the diluted samples at 25 or 50 °C for 10 min, followed by addition of glutaraldehyde solution to a final concentration of 1% and incubation at the same temperatures for 30 min. The solutions containing the particles were then dialyzed overnight to dialyzed water at 4 °C to remove unreacted glutaraldehyde. The fixed particles were placed on a carbon-coated copper grid for 10 min at room temperature and stained by negative staining method using phosphotungstate or uranyl acetate for 30 s. Stained samples were dried on filter paper at room temperature for 2 h or more. Grids were examined in H-7500 (Hitachi) TEM at 80 kV. The digital images were acquired with a charge coupled device camera.

Incorporation of 1-Anilinonaphthalene-8-sulfonate. To quantify the incorporation of the fluorescence probe magnesium 1-anilinonaphthalene-8-sulfonate (1,8-ANS) (Nacalai Tesque, Japan) into the nanoparticles, proteins (300 μg/mL) and 1,8-ANS (100 μM) were mixed in PBS followed by incubation at 25 °C for 10 min. The samples were measured in optically clear polystyrene microcuvettes (Bio-Rad, CA) on a fluorescence spectrofluorometer (FP-6500 Jasco, Japan) with an excitation wavelength of 370 nm and an emission wavelength scanning from 400 to 650 nm at 25 °C. Next, the samples were incubated for 10 min at 50 °C and measured again at 50 °C. Finally, the emission spectra at 25 °C were measured again after incubation at 25 °C.

Evaluation of Protein Binding through Coiled-Coil Structure. To show the specific binding between helix A and helix B as well as the optimum concentration of our fusion proteins to be used in further experiments, 96-well ELISA plates (Costar 3361, Corning Life sciences, Lowel, MA) were coated overnight at 4 °C with 250, 500, 750, and 1000 nM of PDB. Plates were washed 3 times with PBS-T and blocked overnight with 2% bovine serum albumin (BSA) in PBS buffer at 4 °C. After blocking, plates were washed again and incubated with 100 nM helixA-scVEGF$_{121}$ for 1 h at 37 °C. After washing, anti-VEGF$_{121}$ (Abcam Life Sciences, Cambridge, MA) was reacted for 1 h at 37 °C. HRP-conjugated secondary IgG at 1:1000 dilution was added and reacted for 1 h at 37 °C. TMB peroxidase substrate (KPL, Gaithersburg, MD) was added after washing three times with PBS-T and reaction was stopped after 5 min by adding 1 N HCl. The binding was detected and measured spectrophotometrically at a wavelength of 450 nm (Benchmark, Bio-Rad).

In Vitro Cytotoxicity. To incorporate PTX into nanoparticles, ELP-D-helixB (1 μM) and PTX (10 μM) in the presence or absence of helixA-scVEGF$_{121}$ (1 μM) were mixed and incubated at 50 °C. After incubation, PTX-loaded protein nanoparticles were dialyzed using a Slide-A-lyzer dialysis cassette against PBS at 37 °C to remove unloaded PTX.

HeLa cells resuspended in Dulbecco's modified eagle medium, DMEM (Wako, Japan) containing 10% FBS and 1% PS were seeded in 35-mm-diameter glass-bottomed culture dish (Iwaki, Japan) at a density of 5×10^4 cells/dish. After cell attachment to the culture dish, PTX-loaded protein nanoparticles were added to cells. The day on which proteins nanoparticles were added was considered as day 0. To evaluate PTX-loaded protein nanoparticle efficacy, cells were stained with calcein-AM (Calcein) for living cells and propidium iodide (PI) for dead cells. Fluorescent images were acquired using fluorescence microscopy (IX-70 Olympus, Japan).

■ ASSOCIATED CONTENT

Supporting Information

Additional figure S1 about induction of cell. The Supporting Information is available free of charge on the ACS Publications website at DOI: 10.1021/acs.bioconjchem.5b00266.

DOI: 10.1021/acs.bioconjchem.5b00266
Bioconjugate Chem. 2015, 26, 1672−1677

AUTHOR INFORMATION

Corresponding Author

*E-mail: kobatake.e.aa@m.titech.ac.jp. Fax: +81 45 924 5779. Phone: +81 45 924 5760.

Notes

The authors declare no competing financial interest.

ACKNOWLEDGMENTS

This work was financially supported by Grants-in-aid for Scientific Research from the Ministry of Education, Culture, Sports, Science and Technology of Japan and JSPS Institutional Program for Young Researcher Overseas Visits. We are also grateful to Ms. Keiko Ikeda from the Technical Department of the Tokyo Institute of Technology for technical support with the transmission electron microscope imaging.

REFERENCES

(1) Urry, D. W., Parker, T. M., Reid, M. C., and Gowda, D. C. (1991) Biocompatibility of the bioelastic materials, poly(GVGVP) and its gamma-irradiation cross-linked matrix - summary of generic biological test-results. *J. Bioact. Compat. Polym. 6*, 263−282.

(2) Herrero-Vanrell, R., Rincon, A. C., Alonso, M., Reboto, V., Molina-Martinez, I. T., and Rodriguez-Cabello, J. C. (2005) Self-assembled particles of an elastin-like polymer as vehicles for controlled drug release. *J. Controlled Release 102*, 113−22.

(3) Betre, H., Liu, W., Zalutsky, M. R., Chilkoti, A., Kraus, V. B., and Setton, L. A. (2006) A thermally responsive biopolymer for intra-articular drug delivery. *J. Controlled Release 115*, 175−82.

(4) Urry, D. W., and Pattanaik, A. (1997) Elastic protein-based materials in tissue reconstruction. *Ann. N.Y. Acad. Sci. 831*, 32−46.

(5) Fujita, Y., Mie, M., and Kobatake, E. (2009) Construction of nanoscale protein particle using temperature-sensitive elastin-like peptide and polyaspartic acid chain. *Biomaterials 30*, 3450−7.

(6) Dreher, M. R., Simnick, A. J., Fischer, K., Smith, R. J., Patel, A., Schmidt, M., and Chilkoti, A. (2008) Temperature triggered self-assembly of polypeptides into multivalent spherical micelles. *J. Am. Chem. Soc. 130*, 687−694.

(7) Matsumoto, R., Hara, R., Andou, T., Mie, M., and Kobatake, E. (2014) Targeting of EGF-displayed protein nanoparticles with anticancer drugs. *J. Biomed Mater. Res. B: Appl. Biomater. 102*, 1792−8.

(8) Parry, D. A., Fraser, R. D., and Squire, J. M. (2008) Fifty years of coiled-coils and alpha-helical bundles: a close relationship between sequence and structure. *J. Struct. Biol. 163*, 258−269.

(9) Boucher, C., Ruiz, J. C., Thibault, M., Buschmann, M. D., Wertheimer, M. R., Jolicoeur, M., Durocher, Y., and De Crescenzo, G. (2010) Human corneal epithelial cell response to epidermal growth factor tethered via coiled-coil interactions. *Biomaterials 31*, 7021−31.

(10) Murschel, F., Liberelle, B., St-Laurent, G., Jolicoeur, M., Durocher, Y., and De Crescenzo, G. (2013) Coiled-coil-mediated grafting of bioactive vascular endothelial growth factor. *Acta Biomater 9*, 6806−13.

(11) Pechar, M., Pola, R., Laga, R., Ulbrich, K., Bednarova, L., Malon, P., Sieglova, I., Kral, V., Fabry, M., and Vanek, O. (2011) Coiled coil peptides as universal linkers for the attachment of recombinant proteins to polymer therapeutics. *Biomacromolecules 12*, 3645−55.

(12) Pola, R., Laga, R., Ulbrich, K., Sieglova, I., Kral, V., Fabry, M., Kabesova, M., Kovar, M., and Pechar, M. (2013) Polymer therapeutics with a coiled coil motif targeted against murine bcl1 leukemia. *Biomacromolecules 14*, 881−9.

(13) Pechar, M., Pola, R., Laga, R., Braunova, A., Filippov, S. K., Bogomolova, A., Bednarova, L., Vanek, O., and Ulbrich, K. (2014) Coiled coil peptides and polymer-peptide conjugates: synthesis, self-assembly, characterization and potential in drug delivery systems. *Biomacromolecules 15*, 2590−9.

(14) Kobatake, E., Takahashi, R., and Mie, M. (2011) Construction of a bFGF-tethered extracellular matrix using a coiled-coil helical interaction. *Bioconjugate Chem. 22*, 2038−42.

(15) Assal, Y., Mie, M., and Kobatake, E. (2013) The promotion of angiogenesis by growth factors integrated with ECM proteins through coiled-coil structures. *Biomaterials 34*, 3315−23.

(16) Mie, M., Sasaki, S., and Kobatake, E. (2014) Construction of a bFGF-tethered multi-functional extracellular matrix protein through coiled-coil structures for neurite outgrowth induction. *Biomed. Mater. 9*, 015004.

(17) O'Shea, E. K., Rutkowski, R., Stafford, W. F., 3rd, and Kim, P. S. (1989) Preferential heterodimer formation by isolated leucine zippers from fos and jun. *Science 245*, 646−8.

(18) O'Shea, E. K., Lumb, K. J., and Kim, P. S. (1993) Peptide 'Velcro': design of a heterodimeric coiled coil. *Curr. Biol. 3*, 658−67.

(19) Boesen, T. P., Soni, B., Schwartz, T. W., and Halkier, T. (2002) Single-chain vascular endothelial growth factor variant with antagonist activity. *J. Biol. Chem. 277*, 40335−41.

(20) McPherson, D. T., Xu, J., and Urry, D. W. (1996) Product purification by reversible phase transition following Escherichia coli expression of genes encoding up to 251 repeats of the elastomeric pentapeptide GVGVP. *Protein Expr. Purif. 7*, 51−7.

(21) De Campos Vidal, B. (1978) The use of the fluorescent probe 8-anilinonaphthalene sulfate (ANS) for collagen and elastin histochemistry. *J. Histochem. Cytochem. 26*, 196−201.

(22) Yui, H., Guo, Y., Koyama, K., Sawada, T., John, G., Yang, B., Masuda, M., and Shimizu, T. (2005) Local environment and property of water inside the hollow cylinder of a lipid nanotube. *Langmuir 21*, 721−7.

(23) Wright, E. R., and Conticello, V. P. (2002) Self-assembly of block copolymers derived from elastin-mimetic polypeptide sequences. *Adv. Drug Delivery Rev. 54*, 1057−73.

(24) Meyer, D. E., Kong, G. A., Dewhirst, M. W., Zalutsky, M. R., and Chilkoti, A. (2001) Targeting a genetically engineered elastin-like polypeptide to solid tumors by local hyperthermia. *Cancer Res. 61*, 1548−54.

(25) Kuwajima, K. (1989) The molten globule state as a clue for understanding the folding and cooperativity of globular-protein structure. *Proteins 6*, 87−103.

(26) Semisotnov, G. V., Rodionova, N. A., Razgulyaev, O. I., Uversky, V. N., Gripas, A. F., and Gilmanshin, R. I. (1991) Study of the ″molten globule″ intermediate state in protein folding by a hydrophobic fluorescent probe. *Biopolymers 31*, 119−28.

(27) Ptitsyn, O. B. (1995) Molten globule and protein folding. *Adv. Protein Chem. 47*, 83−229.

(28) Ban, H. S., Uno, M., and Nakamura, H. (2010) Suppression of hypoxia-induced HIF-1alpha accumulation by VEGFR inhibitors: Different profiles of AAL993 versus SU5416 and KRN633. *Cancer Lett. 296*, 17−26.

DOI: 10.1021/acs.bioconjchem.5b00266
Bioconjugate Chem. 2015, 26, 1672−1677